NASA TECHNICAL NOTE

NASA TN D-3031
C.1

NASA TN D-3031

INVESTIGATION OF A TWISTED CAMBERED WING WITH A 75° SWEPT LEADING EDGE AT MACH 3 AND REYNOLDS NUMBERS TO 39 x 10^{6}

by John A. Moore

Langley Research Center
Langley Station, Hampton, Va.

NATIONAL AERONAUTICS AND SPACE ADMINISTRATION • WASHINGTON, D. C. • OCTOBER 1965

INVESTIGATION OF A TWISTED CAMBERED WING WITH A 75° SWEPT LEADING EDGE AT MACH 3 AND REYNOLDS NUMBERS TO 39×10^6

By John A. Moore

Langley Research Center
Langley Station, Hampton, Va.

NATIONAL AERONAUTICS AND SPACE ADMINISTRATION

INVESTIGATION OF A TWISTED CAMBERED WING WITH A 75° SWEPT LEADING EDGE AT MACH 3 AND REYNOLDS NUMBERS TO 39×10^6

By John A. Moore
Langley Research Center

SUMMARY

Tests were made on a model of a wing designed for a cruise Mach number of 3. The wing had a leading-edge sweep of 75° and was twisted and cambered to produce a maximum lift-drag ratio at a design lift coefficient of 0.1. The tests were conducted at a Mach number of 3.01 and Reynolds numbers based on the mean aerodynamic chord of 10.9×10^6, 20.4×10^6, and 38.9×10^6.

The maximum lift-drag ratio of the wing increased with increasing Reynolds number but was considerably below the values predicted by linear theory. These low values of maximum lift-drag ratio resulted from the fact that the drag-due-to-lift values were larger than the theoretical values and that the minimum drag coefficient, although lower than the theoretical value, occurred at a low value of the lift coefficient. The large values of the drag due to lift seemed to be caused by partial separation of the flow on the upper surface of the wing, which was due to the presence of supercritical flow in this region.

INTRODUCTION

Interest in the design of an aircraft configuration to cruise efficiently at Mach 3 for long distances has led to the investigation of wing planforms with highly swept subsonic leading edges. Linear theory indicated that camber and twist would provide a further reduction in the drag due to lift. (See ref. 1.)

A series of wings based on these concepts was designed at the Langley Research Center. As part of a general program to investigate the drag-due-to lift characteristics of arrow wings with camber and twist, a wing designed for $C_L = 0.1$ at Mach 3 was tested at Reynolds numbers from 1×10^6 to 8×10^6, based on the mean aerodynamic chord, at a Mach number of about 2.9 (refs. 2 and 3). Results of additional tests on improved versions of wings of this series are presented in reference 4, and a summary of the general supersonic wing program is presented in reference 5.

The purpose of the tests reported herein was to extend the test Reynolds number range of the wing investigated in references 2 and 3 to 39×10^6. All tests reported herein were made at a Mach number of 3.01.

SYMBOLS

C_D — drag coefficient, Drag/qS

$C_{D,min}$ — minimum drag coefficient

$C_{D,W}$ — wave drag coefficient, due to thickness

C_L — lift coefficient, Lift/qS

C_{L_α} — lift-curve slope, per degree

C_m — pitching-moment coefficient, Pitching moment/$qS\bar{c}$

$\bar{c}$ — mean aerodynamic chord

K — drag-due-to-lift parameter, dC_D/dC_L^2

L/D — lift-drag ratio

$(L/D)_{max}$ — maximum lift-drag ratio

M — Mach number

p — static pressure, lb/sq ft

q — dynamic pressure, $\frac{\gamma pM^2}{2}$, lb/sq ft

R — Reynolds number based on the mean aerodynamic chord

S — wing area, sq ft

z_u — upper-surface ordinate measured normal to wing reference plane (fig. 2), in.

z_l — lower-surface ordinate measured normal to wing reference plane (fig. 2), in.

α angle of attack, deg

γ ratio of specific heats

ρ distance along wing leading edge from leading-edge apex (fig. 2), in.

σ distance from wing leading edge measured normal to leading edge (fig. 2), in.

APPARATUS

Tunnel and Balance

The tests were made in a 12- by 12.5-inch blowdown jet at the Langley Research Center. The nozzle was designed for $M = 3.12$, and the calibration gave a value of test-section Mach number of 3.01 ± 0.02. Dry air was supplied to the settling chamber at a temperature of 100° F and at a pressure necessary to obtain the desired Reynolds number. The tunnel exhausted to the atmosphere.

Wall mounting was used for the semispan model (fig. 1). The boundary-layer displacement thickness on the nozzle surface in which the wing was mounted was calculated to be 0.4 inch about 6 inches upstream of the wing apex. The boundary layer was removed from this surface with a 1.5-inch-high scoop that spanned the test section 5 inches ahead of the model. Wall suction was provided in the scoop to prevent choking of the scoop passage due to shock-induced separation. In order to determine the effect of the scoop on the flow in the test region, schlieren photographs were taken of the flow with the test section empty and a total-pressure survey of the test region was made. No disturbances were found in the region of the wing.

The balance used to measure the normal and chord forces and the pitching and rolling moments on the wing was of the external, four-component, strain-gage type. The model was supported on the balance by a tang, integral with the model, that projected through the sidewall. A clearance of about 0.005 inch surrounded this projection at the tunnel wall and means were provided to detect fouling during the runs. The box which housed the balance was sealed and evacuated to approximately stream static pressure during the run in order to prevent excessive leakage across the tunnel-wall surface.

The angle of attack was determined with an optical system which employed a small mirror imbedded in the wing surface to reflect a light beam onto recording film.

Model

A sketch of the model tested is given in figure 2 and the ordinates are given in table I. Pertinent data about the model are given in table II. The horizontal reference plane in figure 2, section B-B, is parallel to the direction of the chord force measured by the balance. The angle of this reference plane relative to the direction of the test-section flow is the angle of attack of the model. The reference plane of section A-A in figure 2 is normal to the leading edge. For this wing the maximum thickness distribution as a function of distance along the leading edge is the same as that of the thick, cambered, twisted wing in reference 2, and the wing alone of reference 3.

A wing similar to the cambered arrow-type wing presented in reference 1 is used in this investigation. According to the linear theory of reference 1, the use of large sweepback with subsonic leading edges should produce large reductions in drag due to lift and wave drag due to thickness. The wing is also cambered and twisted to produce a design lift coefficient of 0.1 at Mach 3 by using the superposition method of references 6 and 7 and imposing the condition that drag due to lift be a minimum for the planform. A 63A thickness distribution based on the mean camber line normal to the leading edge was used to determine the surface ordinate. Volume requirements for the design of a long-range bomber determined the overall thickness of the wing.

TESTS AND ACCURACIES

The tests were conducted at a Mach number of 3 and Reynolds numbers based on the mean aerodynamic chord of 10.9×10^6, 20.4×10^6, and 38.9×10^6. The angle-of-attack range was from -8° to 2° $\left(\alpha_{C_{L=0}} \approx -6^\circ\right)$ except at a Reynolds number of 38.9×10^6, where the loads on the model above $\alpha = -4^\circ$ exceeded the limits of the balance.

The model was tested with both free and fixed transition at each Reynolds number. The fixed transition strip was about 1/8 inch wide and was located at approximately $7\frac{1}{2}$ percent of the local chord back from the leading edge on both lower and upper surfaces. The strip was composed of aluminum oxide particles 0.003 to 0.005 inch in diameter; this size was determined from reference 8 as sufficient to cause transition for the test conditions.

Flow on the upper surface of the model was visually determined by using a fluorescent dye mixed with oil painted on the surface and excited with ultraviolet flash lamps. Photographs of the flow on the upper surface of the wing using this technique are shown in figure 3.

The accuracies of the measurements, based on calibration of the nozzle and the balance and angle-of-attack indicator, were determined to be as follows:

M	±0.02
C_L	±0.002
C_D	±0.0005
C_m	±0.002
L/D	±0.2
α, deg	±0.05

Rolling moment was recorded only to correct for interaction forces in the balance.

SUMMARY OF RESULTS

The aerodynamic characteristics of the wing are given in figure 4, where C_D, L/D, α, and C_m are plotted as functions of C_L for various Reynolds numbers. Differences between the data for free transition and the data for fixed transition are small.

The high lift-drag ratios predicted by theory were not attained. The curves of C_D as a function of C_L indicate the reason for this behavior. The variation of C_D with C_L is similar to that predicted by theory and the minimum value of C_D is well below the theoretical value at all Reynolds numbers. However, the rapid rise of C_D at the higher values of C_L causes the curves of L/D to peak at much lower values of C_L than expected. The variation of C_D with $C_L{}^2$ is shown in figure 5 for two Reynolds numbers and the slopes K of these curves are indicated at design C_L. The values of K from 0.83 to 0.86 are much higher than the theoretical value of $K = 0.48$ for this wing. Similar results reported at lower Reynolds numbers (refs. 2 and 3) were attributed to separation on the upper surface of the wing. This separation is believed to result from the interaction of the boundary layer and the shock waves due to supercritical flow over the upper surface of the model. The oil-film photographs in figure 3, taken at a Reynolds number of 20.4×10^6 and at a lift coefficient of 0.1, show this condition to be true at the higher Reynolds numbers of the present tests. The low values of the lift-curve slope $C_{L_\alpha} \approx 0.0167$, compared with a theoretical value of C_{L_α} of 0.0254, are caused by this loss of lift due to shock-induced separation on the upper surface. (See fig. 4.)

The variation of the maximum values of L/D with Reynolds number is shown in figure 6. The values obtained in the present tests agree well with the values for natural transition reported in reference 3 but are much lower than the values predicted by linear theory. Extrapolation of the data to the full-scale Reynolds number of 100×10^6 gives a value of $(L/D)_{max}$ of about 8 compared with the theoretical value of about 9.9.

Figure 7 shows the variation of $C_{D,min}$ with Reynolds number. The values of $C_{D,min}$ obtained in these tests decrease with increasing Reynolds number as expected but are much lower than the values computed by using skin-friction coefficients based on the data obtained by Sommer and Short (ref. 9). The differences may be due somewhat to the theoretical value of the wave-drag coefficient for the wing used in the present investigation; however, since the theoretical value of $C_{D,W}$ is only 0.0025, some of the variation must be due to a low skin-friction drag at the higher Reynolds numbers.

CONCLUDING REMARKS

Results of force tests on a cambered, twisted wing at a Mach number of 3 and Reynolds numbers of 10.9×10^6, 20.4×10^6, and 38.9×10^6 are compared with results from similar investigations made at lower Reynolds numbers. Minimum drag coefficients were lower than the theoretical predictions at the high Reynolds numbers of the present tests, but the minimum values occurred at much lower values of the lift coefficient than predicted by theory. This fact, and the fact that the values of drag due to lift were higher than those predicted by theory, resulted in much lower values of maximum lift-drag ratio than expected. Oil-film studies indicated that this loss of efficiency of the wing was due in part to separation of the flow on the upper surface of the wing.

Langley Research Center,
National Aeronautics and Space Administration,
Langley Station, Hampton, Va., May 7, 1965.

REFERENCES

1. Brown, Clinton E.; and McLean, Francis E.: The Problem of Obtaining High Lift-Drag Ratios at Supersonic Speeds. Jour. Aero/Space Sci., vol. 26, no. 5, May 1959, pp. 298-302.

2. Mueller, James N.; and Grimaud, John E.: Effects of Twist and Camber and Thickness on the Aerodynamic Characteristics of a 75° Swept Arrow Wing at a Mach Number of 2.91. NASA TM X-138, 1959.

3. Hallissy, Joseph M., Jr.; and Hasson, Dennis F.: Aerodynamic Characteristics at Mach Numbers 2.36 and 2.87 of an Airplane Configuration Having a Cambered Arrow Wing With a 75° Swept Leading Edge. NACA RM L58E21, 1958.

4. Hasson, Dennis F.; and Wong, Norman: Aerodynamic Characteristics at Mach Numbers From 2.29 to 4.65 of 80° Swept Arrow Wings With and Without Camber and Twist. NASA TM X-175, 1960.

5. McLean, F. Edward; and Fuller, Dennis E.: Supersonic Aerodynamic Characteristics of Some Simplified and Complex Aircraft Configurations Which Employ Highly Swept Twisted-and-Cambered Arrow-Wing Planforms. Vehicle Design and Propulsion. American Inst. Aero. and Astronautics, Nov. 1963, pp. 98-103.

6. Grant, Frederick C.: The Proper Combination of Lift Loadings for Least Drag on a Supersonic Wing. NACA Rep. 1275, 1956. (Supersedes NACA TN 3533.)

7. Tucker, Warren A.: A Method for the Design of Sweptback Wings Warped To Produce Specified Flight Characteristics at Supersonic Speeds. NACA Rep. 1226, 1955. (Supersedes NACA RM L51F08.)

8. Braslow, Albert L.; and Knox, Eugene C.: Simplified Method for Determination of Critical Height of Distributed Roughness Particles for Boundary-Layer Transition at Mach Numbers From 0 to 5. NACA TN 4363, 1958.

9. Sommer, Simon C.; and Short, Barbara J.: Free-Flight Measurements of Turbulent-Boundary-Layer Skin Friction in the Presence of Severe Aerodynamic Heating at Mach Numbers From 2.8 to 7.0. NACA TN 3391, 1955.

TABLE I.- WING ORDINATES

σ, in.	z_u, in.	z_l, in.
$\rho = 0$		
0	1.1072	1.1072
$\rho = 1.0908$ in.		
0	0.4178	0.4178
.0055	.4396	.4063
.0164	.4609	.4080
.0273	.4794	.4112
.0551	.5149	.4227
.0834	.5519	.4374
.1124	.5879	.4559
.1413	.6218	.4756
.1707	.6594	.4984
.2002	.6992	.5258
.2307	.7450	.5579
.2612	.7990	.5994
.2923	.8710	.6572
$\rho = 2.1816$ in.		
0	0.2160	0.2160
.0109	.2487	.2023
.0218	.2662	.2007
.0436	.2896	.2029
.0551	.3027	.2045
.1107	.3496	.2111
.1385	.3703	.2149
.1953	.4058	.2231
.2242	.4227	.2274
.2531	.4385	.2312
.3114	.4680	.2405
.3709	.4969	.2487
.4003	.5110	.2536
.4309	.5241	.2580
.4914	.5454	.2656
.5847	.5704	.2705

σ, in.	z_u, in.	z_l, in.
$\rho = 3.2724$ in.		
0	0.0987	0.0987
.0164	.1402	.0840
.0327	.1593	.0802
.0491	.1734	.0785
.0824	.1991	.0764
.1238	.2231	.0736
.2078	.2634	.0682
.2503	.2787	.0660
.3796	.3169	.0605
.4232	.3267	.0589
.4674	.3365	.0562
.5558	.3491	.0491
.6010	.3518	.0436
.6916	.3458	.0235
.7374	.3332	.0038
.7832	.3142	-.0235
.8301	.2858	-.0562
.8770	.2536	-.0927
$\rho = 4.3632$ in.		
0	0.0453	0.0453
.0218	.0867	.0251
.0436	.1053	.0185
.0873	.1331	.0071
.1096	.1445	.0027
.1653	.1663	-.0071
.2771	.1953	-.0251
.3338	.2056	-.0349
.3911	.2143	-.0447
.5056	.2225	-.0649
.5644	.2253	-.0753
.6228	.2258	-.0851
.7412	.2214	-.1074
.8012	.2165	-.1194
.9223	.1947	-.1522
.9834	.1756	-.1756
1.1066	.1020	-.2552
1.1688	.0431	-.3136

σ, in.	z_u, in.	z_l, in.
$\rho = 5.4540$ in.		
0	0.0295	0.0295
.0273	.0731	.0049
.0545	.0911	-.0044
.0824	.1042	-.0125
.1374	.1249	-.0273
.2067	.1418	-.0453
.2765	.1522	-.0633
.4172	.1560	-.1004
.4887	.1533	-.1189
.5607	.1489	-.1380
.7052	.1353	-.1773
.7788	.1244	-.1963
.8525	.1118	-.2165
1.0014	.0813	-.2569
1.0766	.0627	-.2782
1.1524	.0409	-.3000
1.3057	-.0191	-.3545
1.4611	-.1173	-.4390
$\rho = 6.5448$ in.		
0	0.0349	0.0349
.0327	.0818	.0109
.0654	.1025	-.0005
.0982	.1162	-.0093
.1314	.1254	-.0180
.2482	.1434	-.0545
.3316	.1423	-.0840
.5007	.1249	-.1418
.5863	.1124	-.1713
.6725	.0965	-.2002
.8465	.0567	-.2552
.9343	.0355	-.2836
1.0226	.0104	-.3120
1.2015	-.0474	-.3671
1.2921	-.0796	-.3949
1.3826	-.1151	-.4232
1.6597	-.2329	-.5072
1.7535	-.2749	-.5345

TABLE I.- WING ORDINATES - Continued

σ, in.	z_u, in.	z_l, in.
ρ = 7.6356 in.		
0	0.0348	0.0348
.0382	.0860	.0091
.0764	.1095	-.0012
.1151	.1231	-.0100
.1538	.1335	-.0198
.1920	.1406	-.0296
.3872	.1438	-.0918
.4854	.1313	-.1289
.6839	.0849	-.2058
.7848	.0566	-.2450
.9877	-.0121	-.3225
1.0903	-.0481	-.3601
1.1552	-.0874	-.3961
1.4022	-.1714	-.4654
1.5075	-.2156	-.4943
1.7207	-.3045	-.5461
1.9367	-.3934	-.5941
2.0458	-.4359	-.6164

σ, in.	z_u, in.	z_l, in.
ρ = 8.7264 in.		
0	0.0291	0.0291
.0436	.0875	.0013
.0873	.1093	-.0085
.1309	.1262	-.0183
.1756	.1387	-.0292
.2198	.1469	-.0396
.3305	.1546	-.0701
.5547	.1311	-.1443
.6681	.1044	-.1880
.7821	.0678	-.2354
.8966	.0258	-.2856
1.0123	-.0211	-.3341
1.1284	-.0718	-.3816
1.3640	-.1814	-.4716
1.4824	-.2370	-.5125
1.6024	-.2921	-.5496
1.8440	-.4001	-.6074
1.9662	-.4530	-.6330
2.2132	-.5479	-.6695
2.3381	-.5834	-.6794

σ, in.	z_u, in.	z_l, in.
ρ = 9.8172 in.		
0	0.0118	0.0118
.0491	.0756	-.0171
.0982	.1029	-.0296
.1478	.1214	-.0411
.2471	.1449	-.0645
.3720	.1514	-.0962
.4974	.1427	-.1343
.6239	.1204	-.1763
.7516	.0904	-.2222
.8797	.0489	-.2712
1.0090	-.0040	-.3236
1.2697	-.1360	-.4360
1.4017	-.2085	-.4932
1.6678	-.3590	-.5952
1.9384	-.4992	-.6716
2.0747	-.5592	-.6988
2.2121	-.6094	-.7152
2.3507	-.6497	-.7217
2.4903	-.6814	-.7196
2.6305	-.7065	-.7097

σ, in.	z_u, in.	z_l, in.
ρ = 10.9080 in.		
0	-0.0177	-0.0177
.0545	.0543	-.0515
.1091	.0826	-.0635
.1642	.1034	-.0766
.2193	.1181	-.0881
.4134	.1361	-.1350
.5530	.1246	-.1748
.6932	.1001	-.2201
.8350	.0635	-.2653
.9774	.0139	-.3155
1.1208	-.0472	-.3690
1.2653	-.1235	-.4273
1.4109	-.2092	-.4895
1.5571	-.2992	-.5479
1.7049	-.3935	-.6089
1.8533	-.4889	-.6657
2.0027	-.5795	-.7147
2.1532	-.6509	-.7475
2.3054	-.7087	-.7682
2.5197	-.7818	-.7829

σ, in.	z_u, in.	z_l, in.
ρ = 11.9988 in.		
0	-0.0563	-0.0563
.0600	.0217	-.0917
.1205	.0528	-.1043
.1805	.0741	-.1168
.2411	.0894	-.1288
.3022	.0992	-.1419
.4543	.1068	-.1757
.6081	.0932	-.2155
.7625	.0643	-.2586
.9185	.0206	-.3055
1.0750	-.0377	-.3540
1.2331	-.1092	-.4064
1.3919	-.1975	-.4642
1.5517	-.2962	-.5259
1.7131	-.4037	-.5913
1.8751	-.5122	-.6578
2.0387	-.6240	-.7249
2.2029	-.7314	-.7855
2.3687	-.8160	-.8247
2.4003	-.8307	-.8318

σ, in.	z_u, in.	z_l, in.
ρ = 13.0896 in.		
0	-0.1016	-0.1016
.0654	-.0181	-.1414
.1314	.0130	-.1517
.1969	.0359	-.1626
.2634	.0523	-.1752
.3294	.0626	-.1872
.4958	.0702	-.2204
.6632	.0512	-.2586
.8323	.0146	-.3001
1.0019	-.0350	-.3443
1.1726	-.1021	-.3906
1.3450	-.1855	-.4408
1.5184	-.2859	-.4975
1.6929	-.3961	-.5581
1.8685	-.5101	-.6257
2.0458	-.6355	-.7004
2.2241	-.7615	-.7778
2.2743	-.7986	-.7997

TABLE I.- WING ORDINATES - Concluded

σ, in.	z_u, in.	z_l, in.
ρ = 14.1804 in.		
0	-0.1526	-0.1526
.0709	-.0702	-.1869
.1423	-.0348	-.1995
.2138	-.0119	-.2109
.2852	.0045	-.2213
.3567	.0143	-.2322
.5372	.0208	-.2633
.7188	-.0004	-.2982
.9015	-.0451	-.3364
1.0853	-.1030	-.3762
1.2707	-.1799	-.4187
1.4573	-.2742	-.4678
1.6449	-.3849	-.5251
1.8342	-.5038	-.5895
2.0245	-.6260	-.6593
2.1369	-.7018	-.7029
ρ = 15.2712 in.		
0	-0.2100	-0.2100
.0764	-.1260	-.2427
.1533	-.0883	-.2547
.2302	-.0649	-.2651
.3071	-.0474	- 2743
.3845	-.0376	-.2841
.5787	-.0344	-.3103
.7739	-.0611	-.3403
.9708	-.1123	-.3769
1.1688	-.1805	-.4069
1.3684	-.2667	-.4429
1.5691	-.3714	-.4903
1.7715	-.4898	-.5514
1.9749	-.6163	-.6196
1.9836	-.6212	-.6223

σ, in.	z_u, in.	z_l, in.
ρ = 16.3620 in.		
0	-0.2678	-0.2678
.0818	-.1827	-.2978
.1642	-.1456	-.3071
.2465	-.1222	-.3147
.3289	-.1064	-.3218
.4118	-.0960	-.3283
.6196	-.0933	-.3485
.8290	-.1287	-.3714
1.0401	-.1876	-.3954
1.2522	-.2662	-.4226
1.4660	-.3589	-.4571
1.6815	-.4691	-.5045
1.8058	-.5350	-.5361
ρ = 17.4528 in.		
0	-0.3324	-0.3324
.0873	-.2506	-.3559
.1751	-.2163	-.3613
.2629	-.1923	-.3657
.3512	-.1770	-.3695
.4390	-.1694	-.3728
.6610	-.1709	-.3821
.8846	-.2141	-.3946
1.1093	-.2812	-.4104
1.3357	-.3646	-.4339
1.5637	-.4595	-.4677
1.5926	-.4666	-.4677

σ, in.	z_u, in.	z_l, in.
ρ = 18.5436 in.		
0	-0.4003	-0.4003
.0927	-.3266	-.4133
.1860	-.2961	-.4139
.2792	-.2737	-.4128
.3731	-.2601	-.4112
.4669	-.2546	-.4090
.7025	-.2644	-.4019
.9397	-.3135	-.4063
1.1786	-.3883	-.4232
1.3237	-.4341	-.4352
ρ = 19.6344 in.		
0	-0.4760	-0.4760
.0982	-.4122	-.4771
.1969	-.3849	-.4689
.2956	-.3669	-.4612
.3949	-.3576	-.4525
.4941	-.3565	-.4432
.7439	-.3734	-.4171
.9577	-.4209	-.4209
ρ = 20.7252 in.		
0	-0.5627	-0.5627
.1036	-.5158	-.5447
.2078	-.4983	-.5223
.3120	-.4934	-.5005
.3545	-.4923	-.4923
ρ = 21.0726 in.		
0	-0.5899	-0.5899

TABLE II.- THEORETICAL PARAMETERS OF CAMBERED TWISTED WING

Design Mach number	3
Aspect ratio	1.79
Sweep, deg	75
Area, sq ft	0.23
Semispan, ft	0.45
Root chord, ft	0.85
Mean aerodynamic chord:	
Length, ft	0.619
Lateral location, distance from center line, ft	0.179
Center of pressure, distance behind apex, ft	0.872
Aerodynamic center, distance behind apex, ft	1.01
Lift-curve slope, per deg	0.02536
Skin-friction coefficient for $R = 10^7$	0.0062

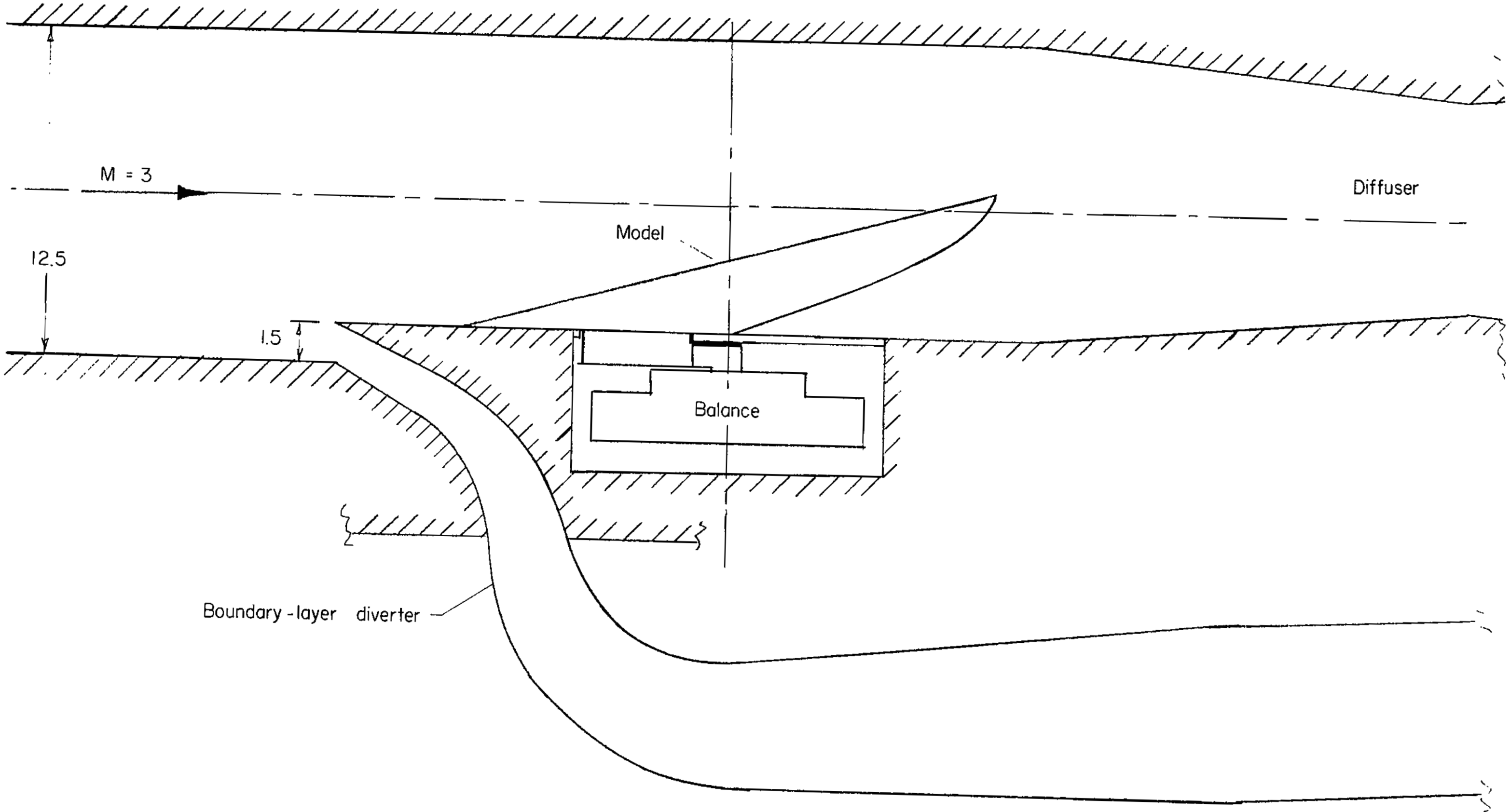

Figure 1.- Schematic drawing of model installation in wind tunnel. All dimensions are in inches.

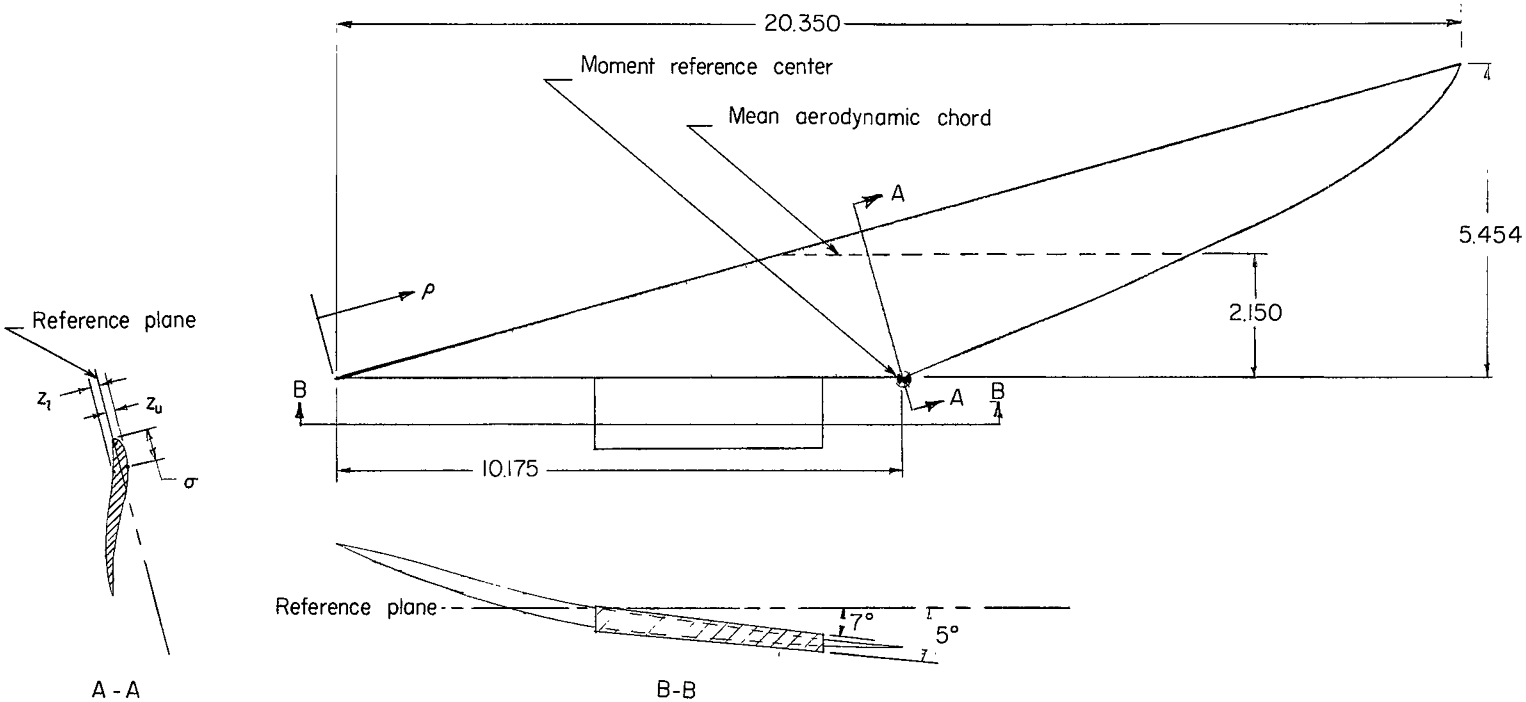

Figure 2.- Schematic drawing of model, showing coordinate system used.
All dimensions are in inches.

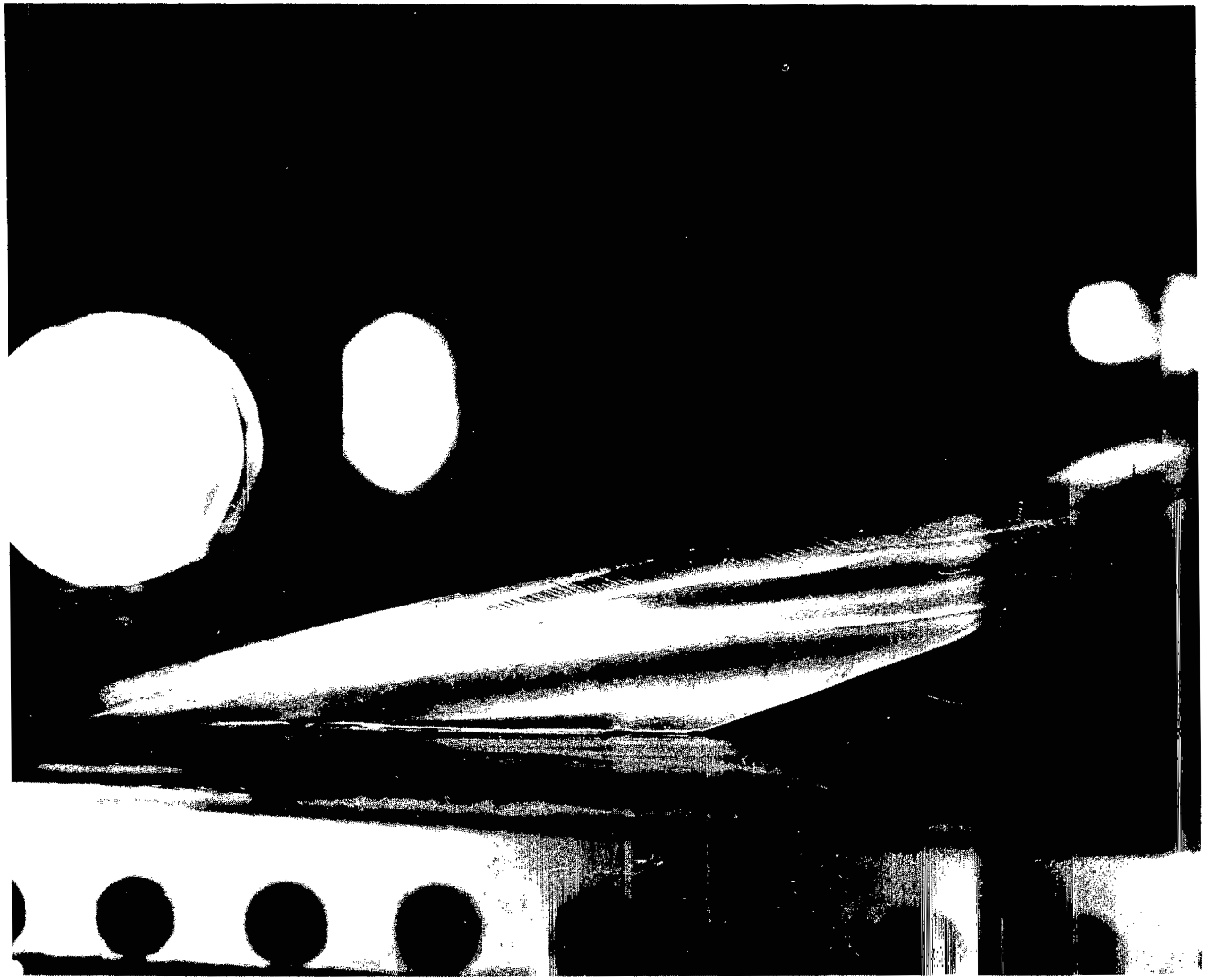

(a) Fixed transition; $C_L = 0.1$; $R = 20.4 \times 10^6$.

L-65-121

Figure 3.- Flow on upper surface of wing using oil-film dye technique.

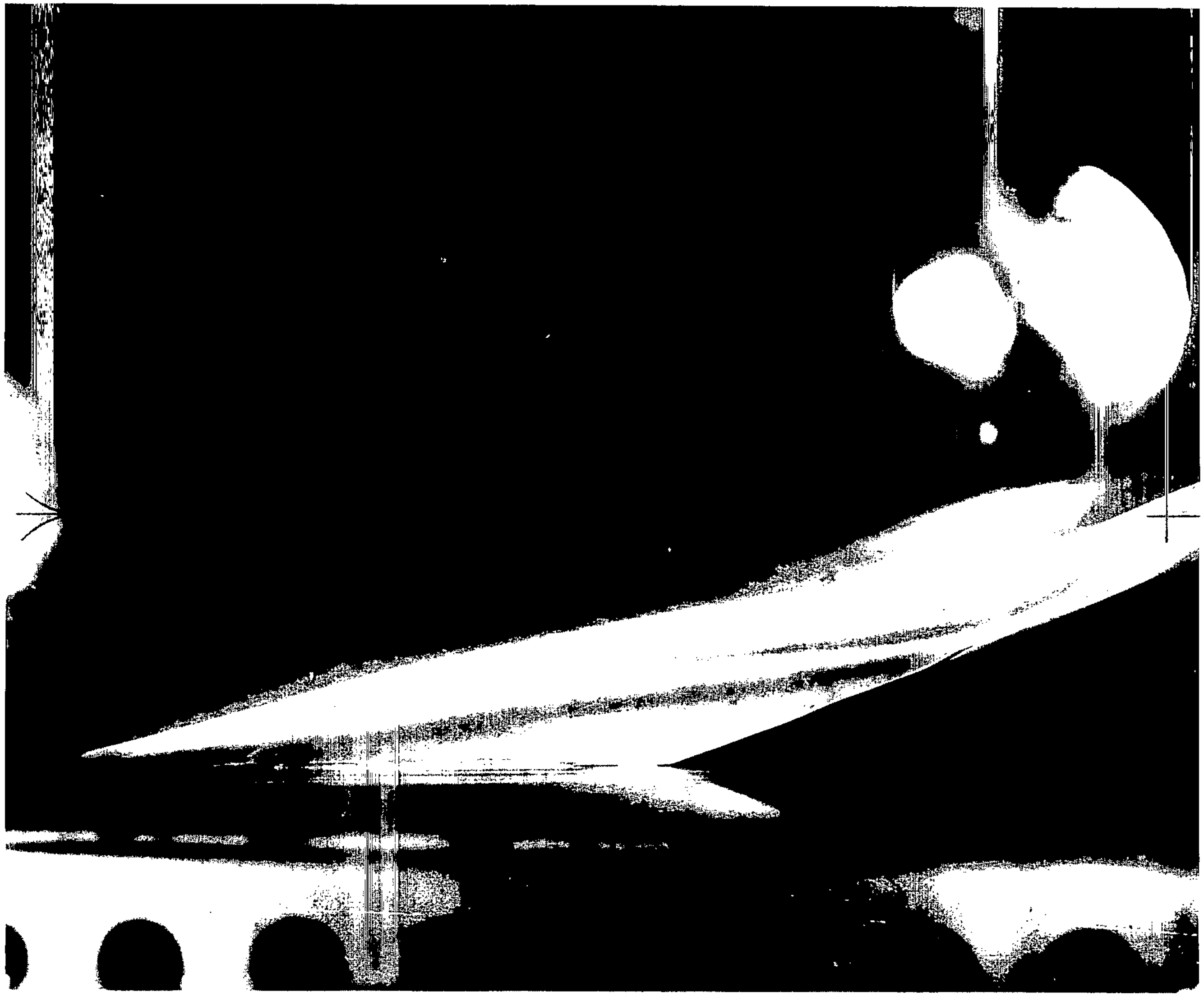

(b) Free transition; $C_L = 0.1$; $R = 20.4 \times 10^6$. L-65-122

Figure 3.- Concluded.

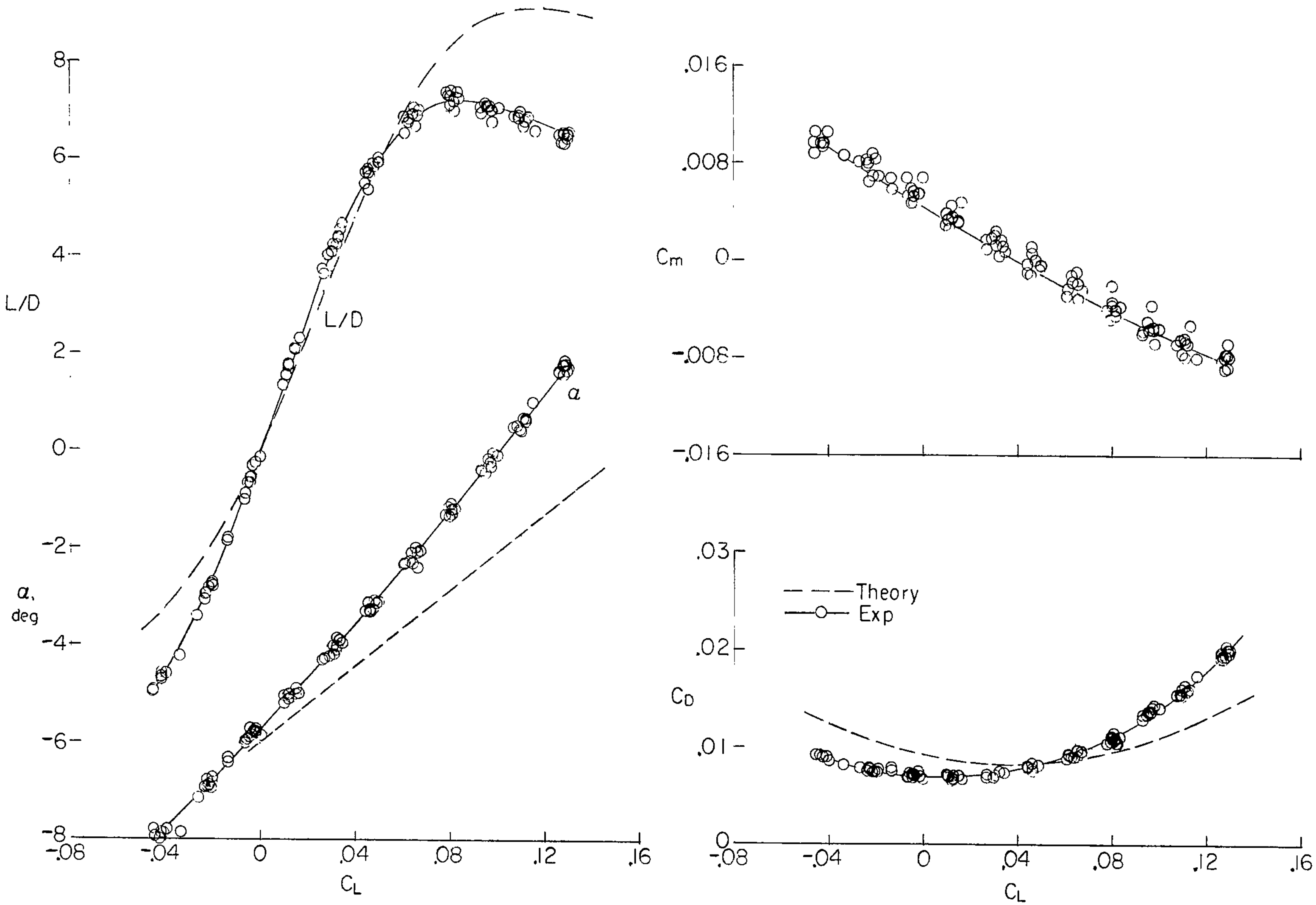

(a) Reynolds number of 10.9×10^6; free transition.

Figure 4.- Aerodynamic characteristics of wing.

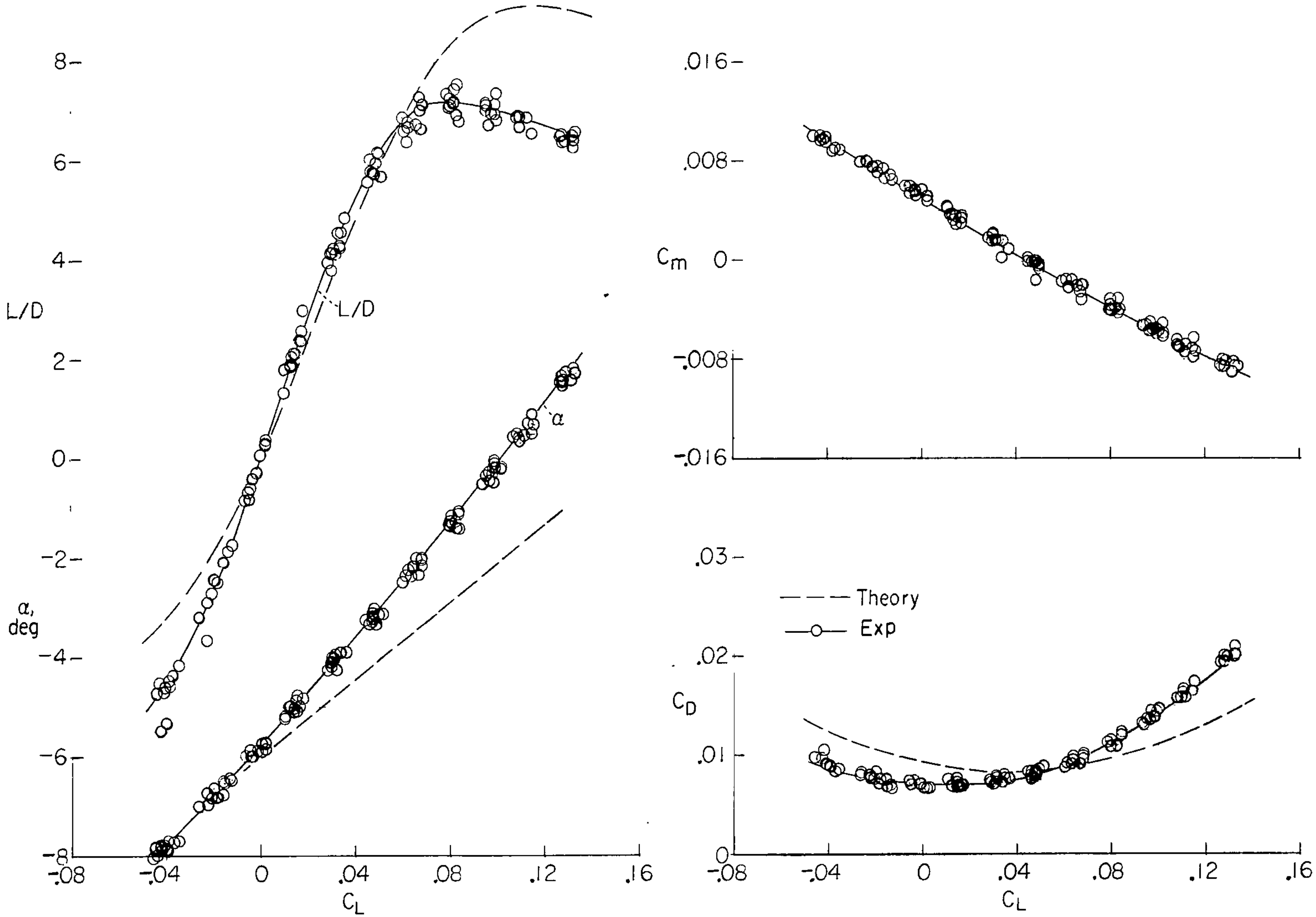

(b) Reynolds number of 10.9×10^6; fixed transition.

Figure 4.- Continued.

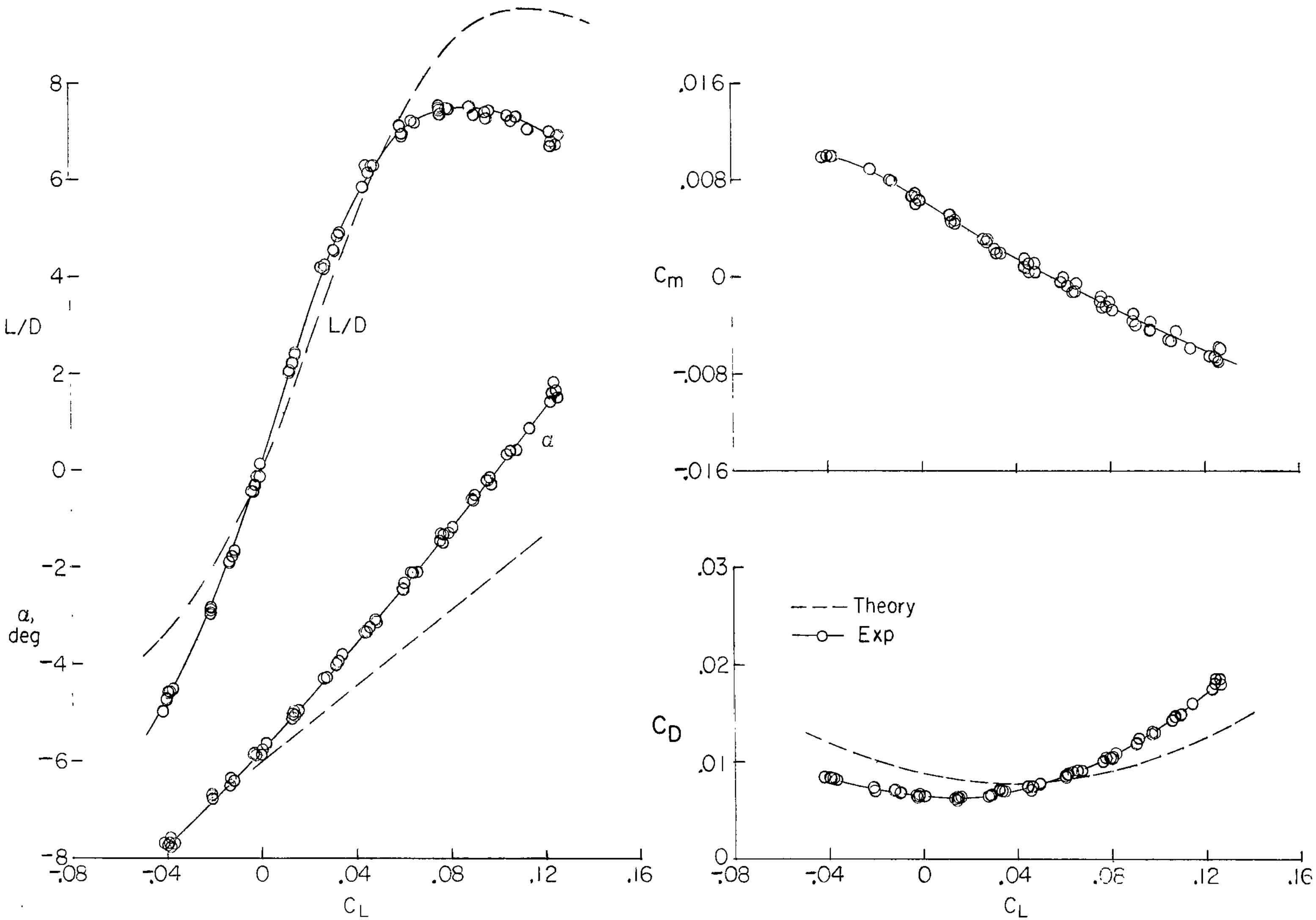

(c) Reynolds number of 20.4×10^6; free transition.

Figure 4.- Continued.

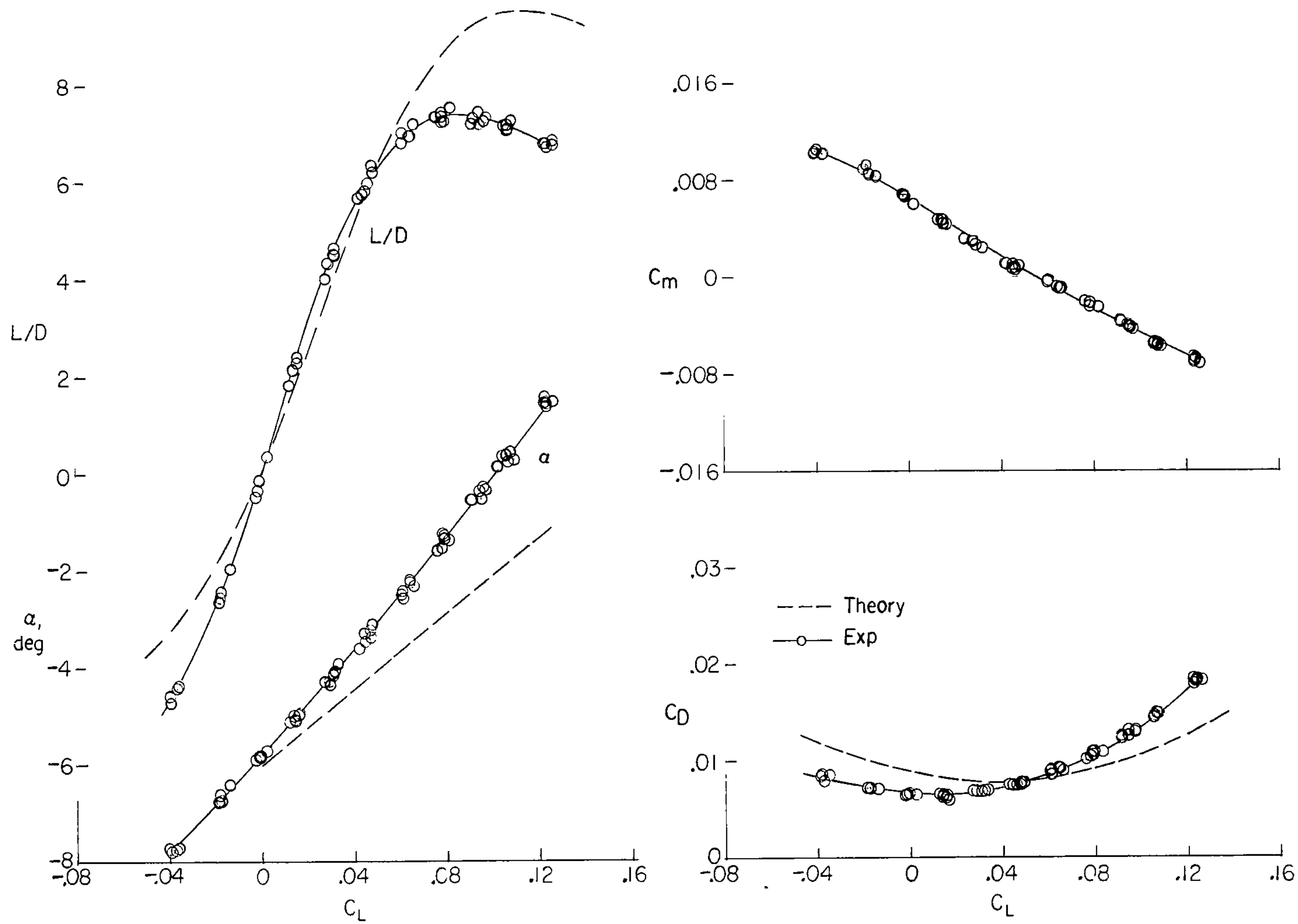

(d) Reynolds number of [illegible].4 × 10^6; fixed transition.

Figure 4.- Continued.

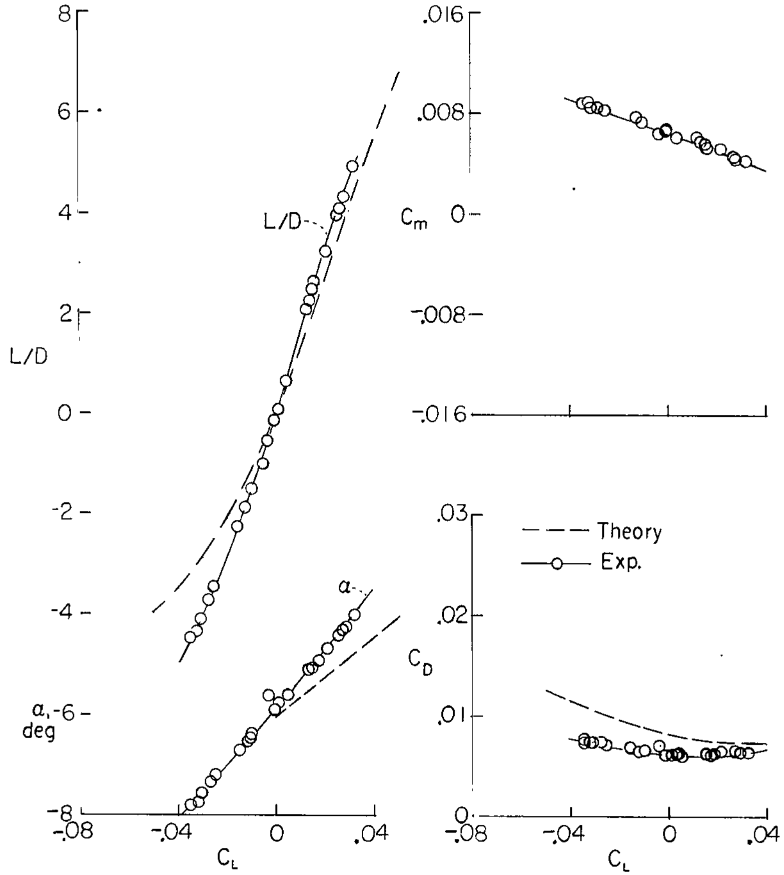

(e) Reynolds number of 38.9×10^6; free transition.

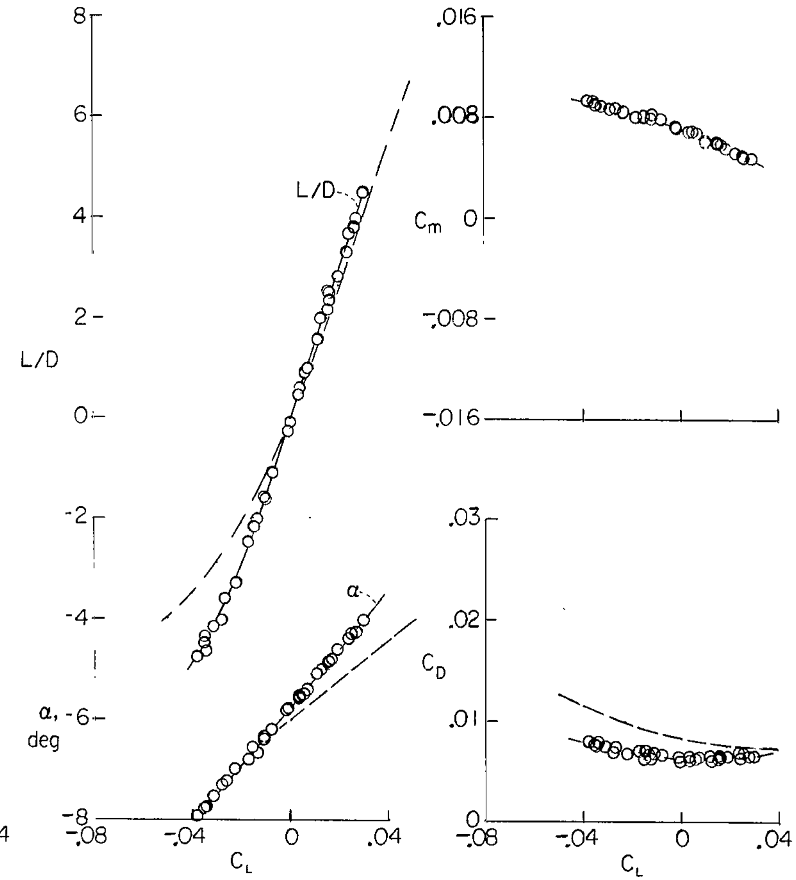

(f) Reynolds number of 38.9×10^6; fixed transition.

Figure 4.- Concluded.

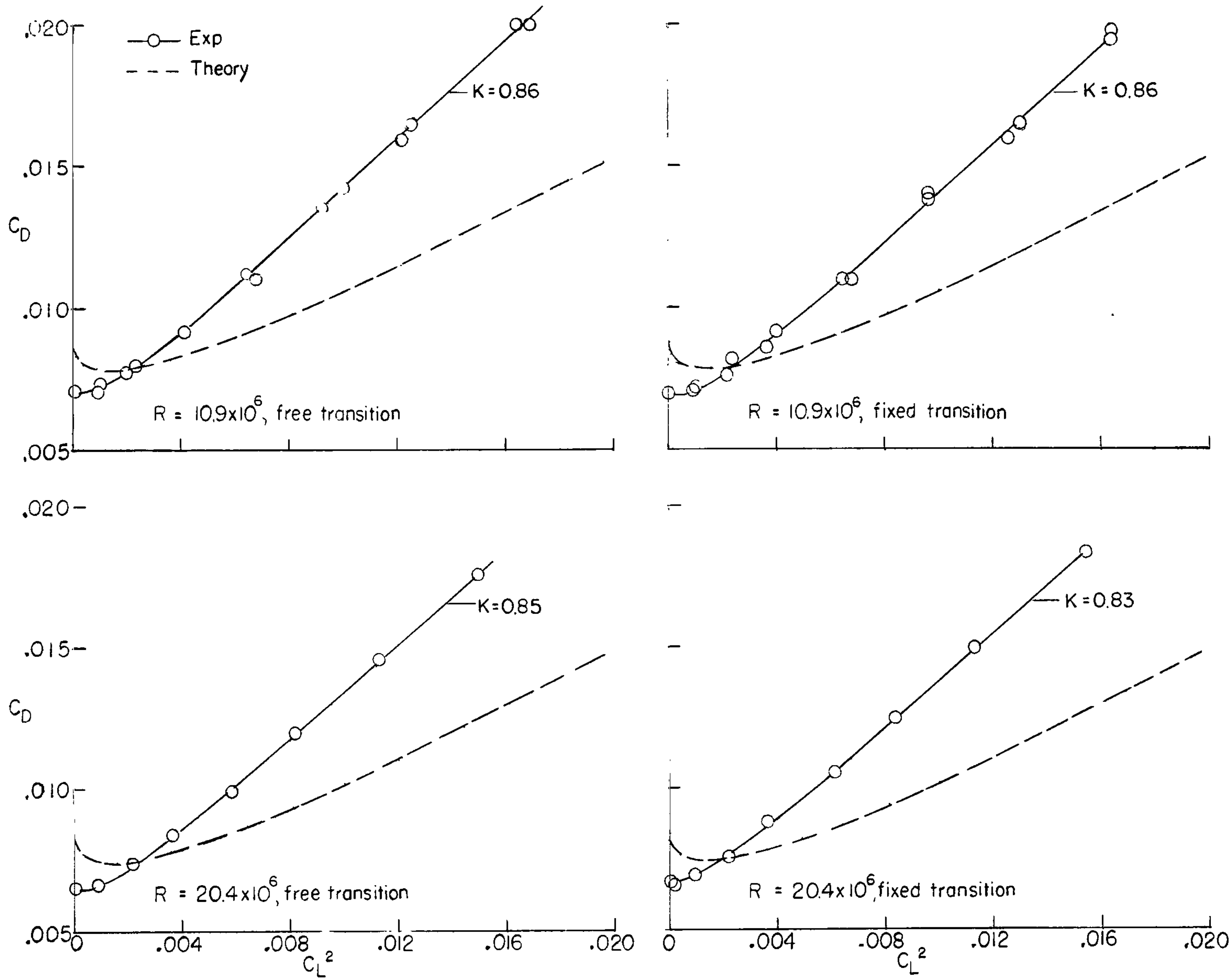

Figure 5.- Variation of drag due to lift.

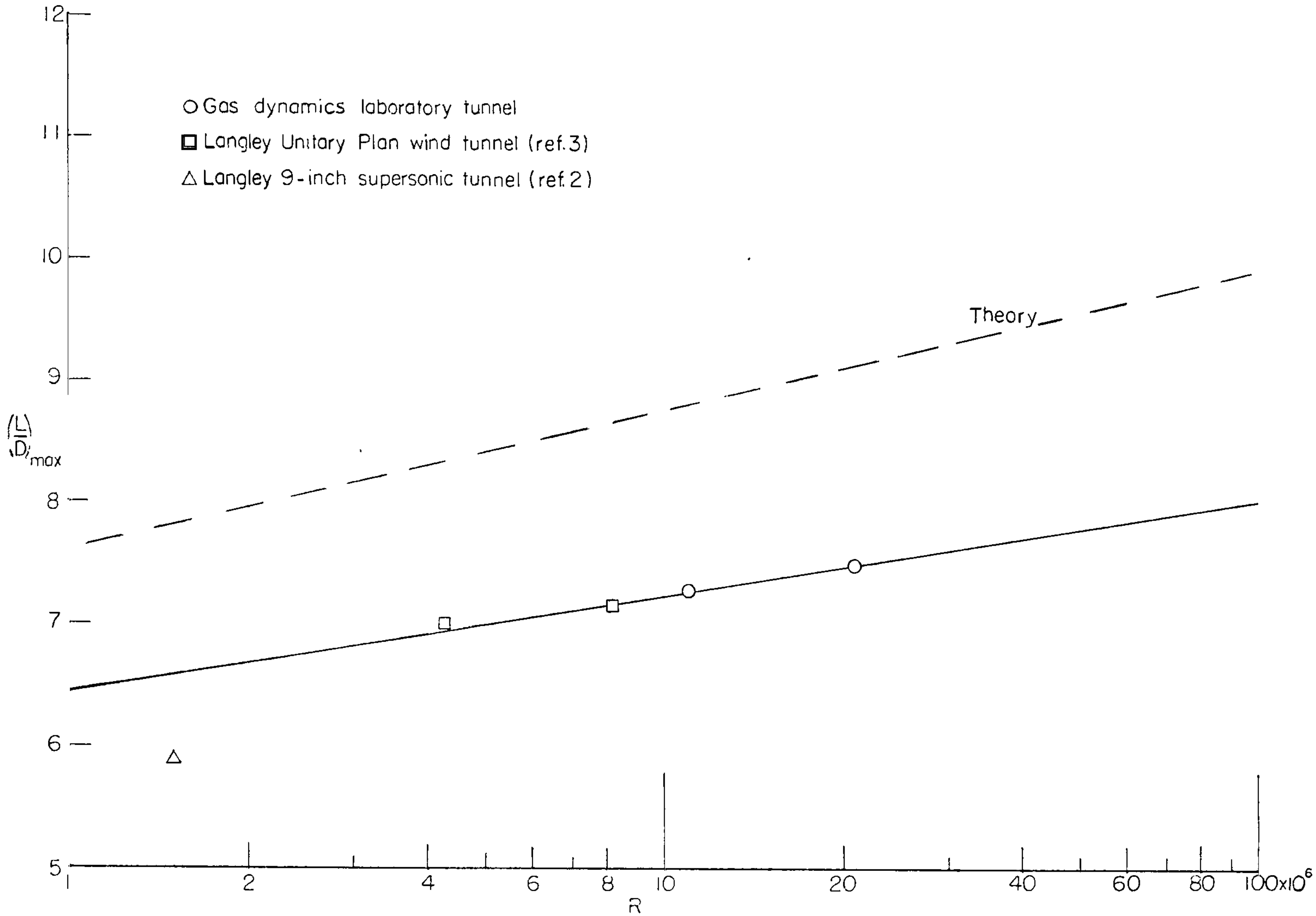

Figure 6.- Variation of maximum lift-drag ratio with Reynolds number.

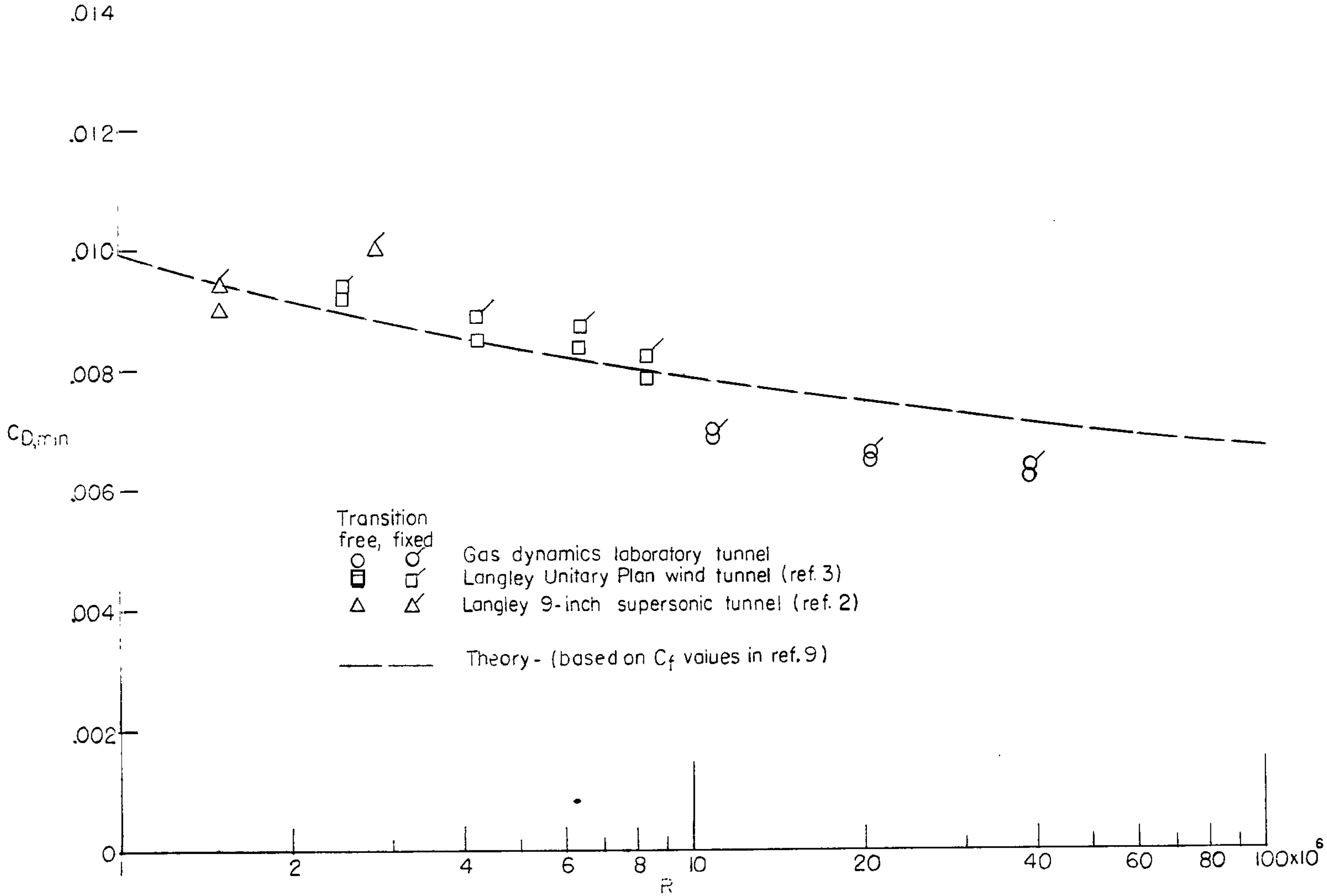

Figure 7.- Variation of minimum drag coefficient with Reynolds number.

NASA-Langley, 1965 L-3504

3 | 1 : | 1 35 8

"The aeronautical and space activities of the United States shall be conducted so as to contribute . . . to the expansion of human knowledge of phenomena in the atmosphere and space. The Administration shall provide for the widest practicable and appropriate dissemination of information concerning its activities and the results thereof."

—NATIONAL AERONAUTICS AND SPACE ACT OF 1958

NASA SCIENTIFIC AND TECHNICAL PUBLICATIONS

TECHNICAL REPORTS: Scientific and technical information considered important, complete, and a lasting contribution to existing knowledge.

TECHNICAL NOTES: Information less broad in scope but nevertheless of importance as a contribution to existing knowledge.

TECHNICAL MEMORANDUMS: Information receiving limited distribution because of preliminary data, security classification, or other reasons.

CONTRACTOR REPORTS: Technical information generated in connection with a NASA contract or grant and released under NASA auspices.

TECHNICAL TRANSLATIONS: Information published in a foreign language considered to merit NASA distribution in English.

TECHNICAL REPRINTS: Information derived from NASA activities and initially published in the form of journal articles.

SPECIAL PUBLICATIONS: Information derived from or of value to NASA activities but not necessarily reporting the results of individual NASA-programmed scientific efforts. Publications include conference proceedings, monographs, data compilations, handbooks, sourcebooks, and special bibliographies.

Details on the availability of these publications may be obtained from:

SCIENTIFIC AND TECHNICAL INFORMATION DIVISION

NATIONAL AERONAUTICS AND SPACE ADMINISTRATION

Washington, D.C. 20546